Open access • Posted Content • DOI:10.1101/2020.07.07.192153

New insights into TNFα/PTP1B and PPARγ pathway through RNF213- a link between inflammation, obesity, insulin resistance and Moyamoya disease — Source link

Priyanka Sarkar, Kavitha Thirumurugan

Institutions: VIT University

Published on: 07 Jul 2020 - bioRxiv (Cold Spring Harbor Laboratory)

Topics: Adipogenesis, Regulatory Pathway, Biological pathway, Insulin resistance and Interactome

New insights into TNFα/PTP1B and PPARγ pathway through RNF213- a link between inflammation, obesity, insulin resistance and Moyamoya disease

Priyanka Sarkar and Kavitha Thirumurugan*

206, Structural Biology Lab, Centre for Biomedical Research, School of Biosciences & Technology, Vellore Institute of Technology, Vellore-632014, India

* m.kavitha@vit.ac.in

Acknowledgements

This work has been financially supported by Vellore Institute of Technology's Seed grant and Senior Research Fellowship by ICMR (Indian Council of Medical Research).

Conflict of interest

The authors declare that they have no conflict of interest.

Abstract

Diabetic patients are always at a higher risk of ischemic diseases like coronary artery diseases. One such ischemic carotid artery disease is Moyamoya. Moyamoya disease (MMD) has been associated with diabetes Type-I and II and the causality was unclear. RNF213 is the major susceptible gene for MMD. To understand the association between diabetes mellitus and MMD we chose the major players from both the anomalies, insulin and RNF213. But before establishing a role of RNF213 in insulin regulating pathway we had to understand the involvement of RNF213 within different biological systems. For this we have adopted a preliminary computational approach to understand the prominent interactions of RNF213. Our first objective was to construct an interactome for RNF213. We have analyzed several curated databases and adapted a list of RNF213 interacting partners to develop its interactome. Then to understand the involvement of this interactome in biological functions we have analyzed major biological pathways, biological processes and prominent clusters related to this interactome through computational approach. Then to develop a pathway that might give clue for RNF213 involvement in insulin regulatory pathway we have validated the intercluster and intracluster predictions and identified a regulatory pathway for RNF213. RNF213 interactome was observed to be involved in adaptive immunity with 4 major clusters; one of the cluster involved TNFα. Immune system involves several pathways, and therefore at this point we have chosen an event-based strategy to obtain an explicit target. Immunity is mediated by many pro-inflammatory cytokines like TNFα. TNFα-mediated inflammation, obesity and insulin resistance are associated. Therefore we chose to explore the role of RNF213 in TNFα-mediated inflammation in macrophages and inflammation-mediated insulin-resistance in adipocytes. We have observed an enhancement of RNF213 gene expression by LPS mediated pro-inflammatory stimuli and suppression by PPARγ-mediated anti-inflammatory, insulin sensitizing stimuli in macrophages. A more significant response

was observed in adipocytes as well. Administration of the pro-inflammatory cytokine TNFα was able to impede the reduction in RNF213 expression during adipogenesis and this effect was observed to be mediated by PTP1B. Inactivation of PTP1B abolished RNF213 expression which in turn enhanced the adipogenesis process through enhanced PPARγ. Constitutive expression of RNF213 suppressed the adipocyte differentiation by the inhibition of PPARγ. We could show the expression of RNF213 has been regulated by TNFα/PTP1B pathway and PPARγ. The constitutive expression of RNF213 during adipogenesis appears to be an adipostatic measure that obese patients acquire to inhibit further adipogenesis. This is verified *in silico* by analyzing the gene expression data obtained from Gene Expression Omnibus database, which showed a higher expression of RNF213 in adipose tissue samples of obese people. Overall this study gives new insights in the TNFα-mediated pathway in adipogenesis and suggests a role of RNF213 in adipogenesis via this pathway.

Keywords: RNF213, *in silico* interactome analysis, TNFα, inflammation, insulin-resistance, PTP1B, PPARγ, adipogenesis

Introduction

Diabetic patients have been marked at a higher risk of coronary artery diseases lead by ischemic injury (Howangyin & Silvestre, 2014). This has made Diabetes mellitus a leading cause for stroke and microvasculature impairments in brain (Ergul, Kelly-Cobbs, Abdalla, & Fagan, 2012). Diabetes has been enormously linked to cerebrovascular diseases (Dalal & Parab, 2002; Zhou, Zhang, & Lu, 2014). Moyamoya disease is an ischemic cerebrovascular disease of carotid arteries. RNF213 (Ring Finger Protein 213) the founder susceptible gene for MMD has been extensively studied to elucidate its role in the pathogenesis of Moyamoya disease (Fujimura et al., 2014; Kamada et al., 2011; Kim, 2016; Shoemaker et al., 2015). MMD is characterized by sprouting of vessels at the base of the brain and stenosis of internal

carotid artery caused by hyperplasia of smooth muscle cells present in the intima of carotid arteries. This is sometimes accompanied by lipid accumulation in the proliferating intima which ultimately leads to occlusion due to reduction in the lumen space of carotid arteries (J. Suzuki & Takaku, 1969; Yamauchi et al., 2000). This is quite similar to the condition observed in Type 2 diabetes complications leading to stroke (Zhou et al., 2014). Further MMD has been associated to type 2 Diabetes mellitus in some reports, through their clinical investigations (S. Suzuki et al., 2011). Study by Hatasu Kobayashi, suggested the involvement of RNF213 in type I Diabetes mellitus. They showed that ablation of RNF213 retarded the progression of diabetes in Akita mice (H. Kobayashi et al., 2013). Akita mice are model for type I Diabetes mellitus with a mutation in Ins2 (Pre-proinsulin 2).

RNF213 is an E3 ubiquitin ligase with AAA^+ ATPase domain and a RING domain to perform the ligase activity (Morito et al., 2014). Though most of the previous studies had focused on its physiological and clinical aspects, few independent studies suggested potential regulatory mechanism for RNF213. Study by Scholz suggested RSPO3 (R-spondin3) as a co-regulatory gene for RNF213 (Scholz et al., 2016). Another study by Kazuhiro Ohkubo suggested that RNF213 is transcriptionally activated by the synergistic effect of TNFα and IFNγ in endothelial cells, and PKR and PI3K-AKT pathways act as upstream regulators for these cytokines. Also they revealed the involvement of RNF213 in inflammation through detailed analysis of curated datasets (Ohkubo et al., 2015). It is still not known whether these cytokines directly regulate the transcription of RNF213 or indirectly through some downstream regulators. Further, RNF213 protein was reported to be a substrate for PTP1B (Banh et al., 2016). PTP1B is a negative regulator of insulin (Nieto-Vazquez et al., 2007). TNFα is also known to cause insulin resistance (Lorenzo et al., 2008). It also acts as an anti-adipogenic factor in a way through altering PTP1B (D. D. Song et al., 2013). Also, these cytokine-mediated pro-inflammatory molecules are secreted by activated macrophages.

When a host is invaded by a pathogen, dendritic cells are the first to get triggered, followed by macrophages. Activated macrophages and dendritic cells act as effector phase molecule for the adaptive immunity by engulfing, processing and presenting the antigens on its surface to T_H cells and activates inflammation (Cronkite & Strutt, 2018; Janeway, P, M, & Al., 2001; N. F. and K. Kobayashi, 2005). Inflammation has been extensively studied in relation to obesity. Though obesity is stated as a low grade inflammation, pro-inflammatory cytokines are known to act as negative regulators for adipocyte differentiation.

All these studies gave valuable insights about the regulatory mechanism that might cue the involvement of RNF213. But a detailed analysis of the plausible interactome for RNF213 has not been performed.

Therefore, we have adopted an *in silico* approach to predict an interactome for RNF213. Gene co-regulatory and gene ontology studies have always been valued for predicting the functional attributes of a gene. Several tools are available online to predict accurate hits which can further be screened and validated and we applied this methodology as a base for our study. Based on these findings we have designed the study to validate some of our *in silico* predictions and explored new insights into an already existing anti-adipogenic insulin regulatory pathway.

Results and Discussion

In silico analysis

The predicted interactome of RNF213 (Figure 1) was observed to be involved in several biological systems (Figure2a) but mainly involved in immunity and cytokine driven bioprocesses (Figure 2b) among which MHC Class1 antigen processing and presentation in immune system was the major hit (Figure 2c). There were four major gene clusters (Figure

3a) observed to be functioning within the interactome. One of the clusters belongs to RNF213 and it had 12 members including RNF213. Among the observed list of proteins, DTX3L, TRIM21 and HERC6 were co-regulated with RNF213 (Supplementary data 3). Each cluster belongs to members having similar function within a biological system. Among these 4 clusters, other 2 clusters belong to members involved in inflammation and host defense immune responses. One cluster included NOTCH1 (Fazio & Ricciardiello, 2016; Toshihiro Ito, Judith M. Connett, Steven L. Kunkel, 2012) and the other cluster belong to TNFα and PTP1B (G. J. Song et al., 2016; Zabolotny et al., 2008). The fourth cluster represented the ATP synthase members. Macrophages were selected as *in vitro* model to validate the *in silico* predictions. Macrophages are the key effectors and modulator cells of immune system (Martinez & Gordon, 2014). Raw 264.7 murine macrophages were chosen because they are activated on encountering pathogens similar to dendritic cells. Macrophages engulf these pathogens and digest the antigen into smaller peptides which are presented to $CD8^+$ T cells on MHC class I molecules (Cronkite & Strutt, 2018). Macrophages are also known to secrete inflammatory molecules and trigger inflammation directly (Janeway et al., 2001; N. F. and K. Kobayashi, 2005). Therefore, macrophages were chosen as an efficient model for intercluster and intracluster validation.

Intercluster and intracluster validation

Raw 264.7 cells were stimulated with LPS. LPS induces classical activation of macrophages (Martinez & Gordon, 2014) by enhancing the secretion of pro-inflammatory cytokine, TNFα (Reis et al., 2012; Soromou et al., 2012). When these cells were treated with LPS, it induced the expression of RNF213 at transcriptional level. Expression of TNFα and RNF213 was pronounced after six hours of activation with LPS (Figure3**b**). Along with this, the co-regulated members of RNF213 cluster were also analyzed to check whether they too show

similar expression profile on LPS stimulation. Interestingly, HECT and RLD domain containing E3 ubiquitin protein ligase family member 6(HERC6), Tripartite motif-containing protein 21 (TRIM21), Deltex E3 Ubiquitin Ligase 3L (DTX3L) displayed a similar expression profile (Figure3**c**) to that of RNF213 and TNFα (Fig.3**b**). Thus members of RNF213 cluster were properly grouped as they were regulated in a similar fashion by the inflammatory stimulus, thereby validating the intra-cluster grouping. In contrast to the co-regulated genes, F-box/LRR-repeat protein 7 (FBXL7) though being a member of the same cluster had some variations with respect to the pattern of RNF213 expression pattern (Figure 3**b**). Similarity between TNFα expression pattern from the other cluster and the expression pattern of members of RNF213 cluster, indicates an intercluster interaction. At this stage we have concluded that TNFα individually might also be able to regulate RNF213.

TNFα is stated as an interlinking node between insulin resistance, obesity and inflammation. It mediates Wnt and inflammation signaling to prevent adipocyte differentiation (Gustafson & Smith, 2006) in 3T3-L1 by suppressing adipogenic genes (Ruan, Hacohen, Golub, Parijs, & Lodish, 2002) and also by impeding the reduction of PTP1B (D.D. Song et al., 2013).

RNF213 Expression in Adipocytes

Therefore to link inflammation and adipogenesis we have attempted to evaluate the expression of RNF213 in adipocytes. We observed RNF213 was expressed well during the first 2 days of adipocyte differentiation and on the 8th day (Figure 4a). There was an inclined suppression of RNF213 expression from 4^{th} day onwards up to 6^{th} day. This is the time when the preadipocyte differentiate into mature adipocytes. In parallel to the regulation of RNF213 we also profiled PTP1B expression that was observed to be similar to that of RNF213 expression during adipocyte differentiation (Figure 4b). This suggested an involvement of major adipogenic regulators like PPARγ and CEBPα in RNF213 regulation. Therefore, we

have evaluated the effect of relation between RNF213, PPARγ and CEBPα expression pattern. CEBPα was not considered for further analysis because it was not synchronized with the expression profile of RNF213 (data not shown). Therefore, we have evaluated the effect of PPARγ on RNF213.

Suppression of RNF213 by PPARγ agonist

PPARγ is a master regulator of adipogenesis and it is activated by thiazolidinediones. Here we have administered pioglitazone. Pioglitazone is not only an activator of PPARγ but it also acts as an anti-inflammatory molecule by suppressing TNFα expression both at protein and mRNA level by activating PPARγ and inactivating NFκB (Ao et al., 2010). It also suppresses the expression of IFNγ in a PPARγ dependent manner(Cunard et al., 2019). Further it decreases the insulin resistance (Kemnitz et al., 1994). Therefore, we have evaluated the effect of pioglitazone treatment in macrophages as well as in adipocytes.

RNF213 was induced by inflammation and slightly suppressed by PPARγ dependent anti-inflammation in macrophages (Figure 5a). Pioglitazone acted as an anti-inflammatory molecule by completely suppressing the expression of TNFα (Figure 5a). Further, there was a significant reduction in the mRNA expression of RNF213 in pioglitazone treated 3T3-L1 adipocytes (Figure 5b). These results indicate insulin sensitivity and anti-inflammation might negatively regulate RNF213 gene expression. We did not use PPARγ inhibitor or PPARγ -RNAi at this stage because we wanted to evaluate the RNF213 expression pattern throughout the adipogenesis process. But inhibiting PPARγ will block adipogenesis.

Effect of TNFα on RNF213 expression

We have attempted to evaluate the effect of pro-inflammatory, negative regulator of insulin, TNFα on RNF213 expression. For this , 3T3-L1 pre-adipocytes were treated with TNFα at an

inflammatory dose causing adipostatic effect (Gustafson & Smith, 2006). The treatment of TNFα impeded the reduction of RNF213 mRNA throughout adipogenesis (Figure 6a). We again performed a parallel expression profiling for PTP1B. We observed a similar pattern in PTP1B expression to that of RNF213 expression (Figure 6b). The same trend was seen in the protein expression of RNF213 and PTP1B following TNFα treatment (Figure 7a-e). Immunostained adipocyte cells were observed for RNF213 and PTP1B expression at day 2 and day 5 of differentiation. The cells treated with TNFα expressed RNF213 and PTP1B throughout adipogenesis process (Figure 7a-d).

Effect of PTP1B on RNF213 expression

Further we wanted to investigate the mechanism followed by TNFα. Since PTP1B was reported as one of the downstream partners of TNFα insulin resistance pathway and in our data also it showed similar trend of expression to that of RNF213 expression. We have evaluated the effect of PTP1B on RNF213. For this we have analysed the effect of PTP1B inactivation on RNF213 expression. The administration of sodium orthovanadate (phosphatase inhibitor) at 35 μM suppressed the mRNA expression of RNF213 (Figure8a). Whereas using PTP1B inhibitor TCS401 specifically at 0.29 μM concentration abolished the expression of RNF213 at gene level (Figure 8b) and protein level. This was indicated by *in vitro* protein expression analysis measured with fluorescently labelled antibodies (Figure7f). Further when TNFα treated cells were co-treated with TCS401, it nullified the TNFα mediated enhanced effect on RNF213 expression (Figure 7e). Day 8 adipocytes treated with TNFα show reduced adipogenesis indicated by less number of Oil Red O stained lipid droplets (Figure 9a-ii) and PPARγ transcript levels (Figure 9b) . Same cells with TCS401 co-treatment show enhanced number of lipid droplets suggesting the role of PTP1B on adipogenesis (Figure 9a-iii).

This indicated that TNFα can also regulate RNF213 and it is mediated through PTP1B. This data showed a complete regulatory dependence of RNF213 on PTP1B.

Effect of positive regulators of RNF213 (TNFα and PTP1B) on PPARγ

Since RNF213 expression was observed to be suppressed by activation we wanted to analyze the effects of positive regulators of RNF213 on PPARγ, the negative regulator of RNF213.

First we have evaluated the gene expression pattern of PPARγ in normal differentiating cells and then compared it with the TNFα treated differentiating cells and PTP1B inhibited differentiating cells. Gene expression of PPARγ was high in adipocytes treated with DIM (differentiation induction media) particularly at day 8 (Figure 9b). PPARγ expression was very low in the cells treated with TNFα. This effect was reversed in cells treated with PTP1B specific inhibitor TCS401 (Figure 9b), the downstream partner of TNFα. This shows that administration of TNFα suppresses PPARγ in the presence of PTP1B. TNFα affects several adipogenic molecules through different pathways. Therefore PPARγ could be acting downstream to PTP1B or it might have its own regulatory pathway to modulate RNF213 expression.

The inactivation of PTP1B individually also increased adipogonesis as indicated by the increased number of lipid droplets (Figure 10) and PPARγ expression levels (Figure 9b). Therefore PTP1B might be regulating RNF213 through PPARγ and further analysis is required to evaluate this mechanism.

Gene expression analysis from Microarray database

Our data suggest the involvement of RNF213 in adipocyte differentiation. This is in accordance to the gene expression data curated from Gene Expression Omnibus through GEO2R tool, where we can observe a 4.5 fold increase in RNF213 expression in non-diabetic

obese PIMA individuals (Supplementary data 4). This was the only curated normalized dataset available that significantly recognized RNF213.

Most of the other datasets had variable probes for RNF213 with unreliable Padj values. Therefore we chose this dataset for our evaluation. Obesity is said to be a low grade/chronic inflammation which leads to insulin resistance (Choi & Cohen, 2017). An increase in the gene expression of RNF213 during obesity suggests its role in obesity related insulin resistance and predicts its likely protective effect in obese patients by reducing adipogenesis.

Perspectives and Conclusion

It is decisive to mark the interacting partners for the gene to know the exact role and the regulatory mechanism of a gene. RNF213 is observed to be present across many uncurated datasets, making it relevant to list the plausible interactors. By curating such datasets we have observed that RNF213 shows an increased gene expression during obese conditions. RNF213 has been reported to be induced by inflammatory stimuli (Ohkubo et al., 2015) and its ablation improves glucose tolerance (H. Kobayashi et al., 2013). These reports are in accordance with our study showing the induction of RNF213 expression by TNFα/PTP1B inflammatory pathway leading towards adipostatic effects. This pathway is known to be involved in insulin resistance in adipocytes (Lorenzo et al., 2008). Our data also shows the continuous expression of RNF213 downstream to PTP1B suppresses adipogenesis. But its ablation by PTP1B inactivation increases adipogenesis. Further there is a cyclic pattern of RNF213 expression suggesting the existence of a feedback inhibition mechanism to regulate RNF213. In this study, we had predicted a whole curated interactome for RNF213 which is partly validated. This prediction highlighted the emerging role of RNF213 in inflammation and inflammation mediated anti-adipogenesis. Also we had speculated that TNFα/PTP1B pathway positively regulates RNF213 expression and negatively regulates adipogenesis.

Further RNF213 knockdown analysis is required to confirm the influential role of RNF213 in TNFα/PTP1B mediated insulin resistance and adipostasis.

From our data it was clear that a reduction in RNF213 expression was required to achieve adipogenesis and this reduction was caused by the activation of PPARγ; indicating PPARγ as an effective regulator of RNF213. RNF213 is expressed in both macrophages as well as adipocytes. Both these cell types are related to inflammation. TNFα looks like the common regulator of RNF213 via PTP1B but PPARγ appears to be more effective in suppressing RNF213 in adipocytes suggesting a link between adipogenesis, insulin resistance, inflammation and MMD via TNFα, PTP1B, PPARγ and RNF213. PTP1B might be inactivating PPARγ in order to induce RNF213, and TNFα and PTP1B is known to suppress PPARγ. Further analysis is required to state whether PPARγ modulates RNF213 through this pathway or some other pathway. Overall TNFα/PTP1B insulin-resistant pathway enhances RNF213 expression whereas PPARγ mediated insulin sensitization suppresses its expression. Therefore RNF213 could be another link between obesity, inflammation, insulin resistance and MMD like TNFα.

Methods

Interactome prediction

A molecular interactome was predicted using protein interactors and gene interactors. Interacting genes were listed down from UCSC Genome Browser's gene interaction tool and GeneMania. Protein-protein interactions were based on literature survey, physical interactors, co-expressed partners and functional homology transfers. Physical interactors and co-expressed partners were sorted through GeneMania and STRING. The functional homologs were detected through Genedecks online web tool. These homologous functional partners were sorted based on domain matching and the protein interactors for these partners were

284 listed as homology transfer interactions. All the interactions were sorted based on their
285 probability matching and false discovery rate (FDR). The value 0.01 was considered as a
286 cutoff for FDR. List of these molecules (Supplementary data 1) were used to predict a
287 molecular interactome dataset and it was uploaded on STRING database to develop a visual
288 interacting network with high confidence (0.7). A diagrammatic representation of this
289 approach has been given in the attachments as flow chart for interactome prediction.
290

291 **Interactome validation and pathway prediction**

292 The obtained interactome dataset was submitted to METASCAPE to obtain enrichment
293 cluster analysis and functional complexes through EXPRESS Analysis. METASCAPE results
294 were verified through DAVID. Members of the interactome dataset were submitted to
295 REACTOME to confirm the biological systems and pathway analysis. These results were
296 confirmed through KEGG PATHWAY by considering the KEGG ontology terms for these
297 molecules. The major complexes as presented by the use of MCODE algorithm were based
298 on the top non-redundant enriched terms from METASCAPE and the biological system
299 pathway from REACTOME. The members of these complexes were analyzed for their co-
300 regulation through Database of Gene Co-Regulation (dGCR) (Williams, 2015) and validated
301 for their co-regulated expression and ligand stimulated regulatory pathway in cell lines.
302

303 **Cell culture**

304 RAW 264.7 cells and 3T3-L1 cells were bought from NCCS (Pune) cell repository, India.
305 RAW 264.7 cells were cultured in DMEM (Himedia) and 10% FBS (Invitrogen, USA) media
306 containing 1% antibiotic-antimycotic solution (100X, Gibco) as described previously
307 (George, Ramasamy, & Sirajudeen, 2019). The 3T3-L1 pre-adipocytes were grown as
308 previously described (Shihabudeen, Roy, James, & Thirumurugan, 2015). Briefly, cells were

grown for 2 days post confluence in DMEM (Invitrogen, USA) supplemented with 10% new born calf serum (Invitrogen, USA). Differentiation was then induced by changing the medium to DMEM supplemented with 10% fetal bovine serum, 0.5 mM 3-isobutyl-1-methylxanthine, 1 µM dexamethasone, and 1.2 µM insulin (Sigma-Aldrich, USA). After 48 h, the differentiation medium (referred to as DIM) was replaced with maintenance medium containing DMEM supplemented with 10% fetal bovine serum and 1.2 µM insulin for 48 hours post induction. Thereafter maintenance medium was replaced every 48 h until 14 days. Cells were incubated at 37°C in a 5% CO_2 environment.

Treatment and sample collection

Raw 264.7 cells were treated with 1µg/ml of LPS to induce inflammation. These cells were collected at different time points; post induction (1h, 3h, 6h, 12h and 24h) and gene expression for the samples were normalized against samples from un-induced Raw 264.7 cells. PPARγ activation for these cells was done by treating the cells with 10µM concentration of pioglitazone.

Samples for 3T3-L1 cells were collected at different time points after inducing with differentiation media (at hours (h) 0h, 2h, 4h, 7h, 9h, 12h, 24h, 48h, and at days 4, 6, 8, 10, 12, 14). Sodium orthovanadate (Sigma) was administered at a concentration of 35 µM as reported previously along with DIM (Liao & Lane, 1995). TNFα (Sigma) was administered at a concentration of 1.5 ng/ml along with DIM and maintenance media up to 12 days. This concentration was chosen based on the previous reports of TNFα causing inflammatory response in 3T3-L1 cells (Gustafson & Smith, 2006).TCS401, specific inhibitor of PTP1B (Veda scientific) (Iversen et al., 2000) was administered at a concentration of 0.29 µM along with DIM and maintenance media up to 8 days. Gene expression for the samples collected at

different time points were normalized against samples from 48 hours pre-induction (referred to as -2 day or control) for 3T3-L1 cells.

Gene expression

Total RNA was isolated using TRIzol reagent according to manufacturer's instructions (Invitrogen, USA). The cDNA was synthesized from 1 µg of total RNA using the Prime script cDNA conversion kit (Takara, India). Gene expression was measured using SYBR green dye (Takara, India) in BIORAD CFX96 Touch Real-Time PCR Detection System. GAPDH was used as an endogenous control in the comparative cycle threshold (CT) method. The list of primers from Xcelris is given in the Supplementary data 2.

Oil Red O staining

Oil Red O staining was performed following a modified protocol previously described (Kraus et al., 2016). Briefly, cells were fixed with 10% formalin for 45 minutes followed by a washing step with 60% isopropanol. Then the cells were air dried and incubated with Oil Red O stain (Sigma) for 30 minutes. Then the cells were washed properly with distilled water and the dried wells were used for imaging. Imaging was done through Olympus Magnus Phase contrast microscope.

Immunocytochemistry

3T3-L1 adipocyte cells were fixed with 4% PFA (paraformaldehyde) for 15 minutes at room temperature, washed with PBS and permeabilized with 0.3 % of TRITON X-100 for 10 min. After blocking the cells with blocking buffer (0.3% TRITON X-100, 1% BSA) for 1 hour; the cells were incubated for 5 hours at 4ºC with specific primary antibody (Alexa488 tagged RNF213 primary antibody and Cy3 tagged PTP1B primary antibody from BIOSS, USA) and

359 then counterstained with DAPI. Samples were collected on day 1, day 2, day 5 and day 7.
360 Imaging was done by using EVOS FLoid imaging station (Thermo Fischer, USA) with 20x
361 fluorite objective and LED light cubes containing hard coated filters (blue, red and green).
362
363 **Gene expression analysis from Microarray database**
364 RNF213 differential expression was re-analyzed in human samples through GEO2R. GEO2R
365 is the R-package offered by Gene Expression Omnibus (GEO) to obtain differentially
366 expressed gene list in a given microarray dataset based on the Fold change and AdjP-values.
367 For this study we have used the dataset accession number GSE2508 from GEO database.
368 GSE2508 dataset comprises of RNA samples isolated from the adipocytes of abdominal
369 subcutaneous fat of non-diabetes Pima Indians (Y. H. Lee, S. Nair, E. Rousseau, P. A.
370 Tataranni, C. Bogardus, P. A. Permana, 2006).
371
372 **Statistical analysis**
373 Each experiment had a lower limit of n=3 (3 biological replicates with 3 technical replicates
374 taken as average).Some experiments were repeated more number of times to confirm
375 accuracy. All data were presented as mean ± SEM. Column statistics and ANOVA was
376 performed using Graphpad Prism v.06 software package. $P< 0.05$ was considered to be
377 statistically significant. It is presented as ns ($p> 0.05$), *($p \leq 0.05$), **($p \leq 0.01$), ***($p \leq$
378 0.001) **** ($p \leq 0.0001$).
379
380 **References**

381 Ao, C., Huo, Y., Qi, L., Xiong, Z., Xue, L., & Qi, Y. (2010). Pioglitazone suppresses the
382 lipopolysaccharide-induced production of inflammatory factors in mouse macrophages

by inactivating NF- k B, *34*, 723–730. https://doi.org/10.1042/CBI20090005

Banh, R. S., Iorio, C., Marcotte, R., Xu, Y., Cojocari, D., Zhang, S., … Habu, T. (2016). PTP1B regulates non -mitochondrial oxygen consumption via RNF213 to promote tumour survival during hypoxia, *18*(7), 803–813. https://doi.org/10.1038/ncb3376.PTP1B

Choi, C. H. E. E. J., & Cohen, P. (2017). How does obesity lead to insulin resistance? *Epigenetics*, 2–3. https://doi.org/10.7554/eLife.30766

Cronkite, D. A., & Strutt, T. M. (2018). The Regulation of Inflammation by Innate and Adaptive Lymphocytes, *2018*.

Cunard, R., Eto, Y., Muljadi, J. T., Christopher, K., Kelly, C. J., & Ricote, M. (2019). Repression of IFN- γ Expression by Peroxisome Proliferator-Activated Receptor γ, *172*, 7530–7536. https://doi.org/10.4049/jimmunol.172.12.7530

Dalal, P. M., & Parab, P. V. (2002). Cerebrovascular disease in type 2 diabetes mellitus. *Neurology India*, *50*(4), 380–385.

Ergul, A., Kelly-Cobbs, A., Abdalla, M., & Fagan, S. C. (2012). Cerebrovascular Complications of Diabetes: Focus on Stroke Adviye. *Endocr Metab Immune Disord Drug Targets*, *12*(2), 148–158. https://doi.org/10.1038/jid.2014.371

Fazio, C., & Ricciardiello, L. (2016). Inflammation and Notch signaling : a crosstalk with opposite effects on tumorigenesis. *Nature Publishing Group*, *7*(12), e2515-7. https://doi.org/10.1038/cddis.2016.408

Fujimura, M., Sonobe, S., Nishijima, Y., Niizuma, K., Sakata, H., Kure, S., & Tominaga, T. (2014). Genetics and Biomarkers of Moyamoya Disease: Significance of RNF213 as a

405 Susceptibility Gene. *Journal of Stroke*, *16*(2), 65–72.
406 https://doi.org/10.5853/jos.2014.16.2.65

407 George, L., Ramasamy, T., & Sirajudeen, K. N. S. (2019). LPS-induced Apoptosis is
408 Partially Mediated by Hydrogen Sulphide in RAW 264 . 7 Murine Macrophages LPS-
409 induced Apoptosis is Partially Mediated by Hydrogen. *Immunological Investigations*, 1–
410 15. https://doi.org/10.1080/08820139.2019.1566355

411 Gustafson, B., & Smith, U. (2006). CYTOKINES PROMOTE WNT SIGNALING AND
412 INFLAMMATION AND IMPAIR THE NORMAL DIFFERENTIATION AND LIPID
413 ACCUMULATION IN Birgit Gustafson and Ulf Smith From the Lundberg Laboratory
414 for Diabetes Research , Department of Internal Medicine , The Sahlgrenska Academy.
415 *JBC Papers*. https://doi.org/10.1074/jbc.M512077200

416 Howangyin, K. Y., & Silvestre, J. S. (2014). Diabetes mellitus and ischemic diseases:
417 Molecular mechanisms of vascular repair dysfunction. *Arteriosclerosis, Thrombosis,*
418 *and Vascular Biology*, *34*(6), 1126–1135.
419 https://doi.org/10.1161/ATVBAHA.114.303090

420 Iversen, L. F., Andersen, S., Branner, S., Mortensen, S. B., Peters, H., Norris, K., … Møller,
421 H. (2000). Structure-based Design of a Low Molecular Weight , Nonphosphorus ,
422 Nonpeptide , and Highly Selective Inhibitor of Protein-tyrosine Phosphatase 1B. *The*
423 *Journal of Biological Chemistry*, *275*(14), 10300–10307.

424 Janeway, C. J., P, T., M, W., & Al., E. (2001). Principles of innate and adaptive immunity.
425 New York: Immunobiology.

426 Kamada, F., Aoki, Y., Narisawa, A., Abe, Y., Komatsuzaki, S., Kikuchi, A., … Kure, S.
427 (2011). A genome-wide association study identifies RNF213 as the first Moyamoya

428 disease gene. *Journal of Human Genetics*, *56*(1), 34–40.
429 https://doi.org/10.1038/jhg.2010.132

430 Kemnitz, J. W., Elson, D. F., Roecker, E. B., Baum, S. T., Bergman, R. N., & Meglasson, M.
431 D. (1994). Pioglitazone increases insulin sensitivity, reduces blood glucose, insulin, and
432 lipid levels, and lowers blood pressure, in obese, insulin-resistant rhesus monkeys.
433 *Diabetes*, *43*(2), 204–211. https://doi.org/10.2337/diab.43.2.204

434 Kim, J. S. (2016). Moyamoya Disease: Epidemiology, Clinical Features, and Diagnosis.
435 *Journal of Stroke*, *18*(1), 2–11. https://doi.org/10.5853/jos.2015.01627

436 Kobayashi, H., Yamazaki, S., Takashima, S., Liu, W., Okuda, H., Yan, J., … Koizumi, A.
437 (2013). Ablation of Rnf213 retards progression of diabetes in the Akita mouse.
438 *Biochemical and Biophysical Research Communications*, *432*(3), 519–525.
439 https://doi.org/10.1016/j.bbrc.2013.02.015

440 Kobayashi, N. F. and K. (2005). Macrophages in Inflammation. *Current Drug Targets -*
441 *Inflammation & Allergy*. https://doi.org/http://dx.doi.org/10.2174/1568010054022024

442 Kraus, N. A., Ehebauer, F., Zapp, B., Rudolphi, B., Kraus, B. J., & Kraus, D. (2016).
443 Quantitative assessment of adipocyte differentiation in cell culture. *Adipocyte*, *5*(4),
444 351–358. https://doi.org/10.1080/21623945.2016.1240137

445 Liao, K., & Lane, M. D. (1995). The blockade of preadipocyte differentiation by protein-
446 tyrosine phosphatase HA2 is reversed by vanadate. *The Journal of Biological Chemistry*,
447 *270*(20), 12123–12132. https://doi.org/10.1074/JBC.270.20.12123

448 Lorenzo, M., Fernández-Veledo, S., Vila-Bedmar, R., Garcia-Guerra, L., De Alvaro, C., &
449 Nieto-Vazquez, I. (2008). Insulin resistance induced by tumor necrosis factor-alpha in

450 myocytes and brown adipocytes. *Journal of Animal Science*, *86*(14 Suppl), E94-104.
451 https://doi.org/10.2527/jas.2007-0462

452 Martinez, F. O., & Gordon, S. (2014). The M1 and M2 paradigm of macrophage activation :
453 time for reassessment, *13*(March), 1–13. https://doi.org/10.12703/P6-13

454 Morito, D., Nishikawa, K., Hoseki, J., Kitamura, A., Kotani, Y., Kiso, K., … Nagata, K.
455 (2014). Moyamoya disease-associated protein mysterin/RNF213 is a novel AAA+
456 ATPase, which dynamically changes its oligomeric state. *Sci Rep*, *4*, 4442.
457 https://doi.org/10.1038/srep04442

458 Nieto-Vazquez, I., Fernández-Veledo, S., de Alvaro, C., Rondinone, C. M., Valverde, A. M.,
459 & Lorenzo, M. (2007). Protein-tyrosine phosphatase 1B-deficient myocytes show
460 increased insulin sensitivity and protection against tumor necrosis factor-alpha-induced
461 insulin resistance. *Diabetes*, *56*(2), 404–413. https://doi.org/10.2337/db06-0989

462 Ohkubo, K., Sakai, Y., Inoue, H., Akamine, S., Ishizaki, Y., Matsushita, Y., … Hara, T.
463 (2015). Moyamoya disease susceptibility gene RNF213 links inflammatory and
464 angiogenic signals in endothelial cells. *Scientific Reports*, *5*(August), 13191.
465 https://doi.org/10.1038/srep13191

466 Reis, J., Guan, X. Q., Kisselev, A. F., Papasian, C. J., Qureshi, A. A., Morrison, D. C., …
467 Qureshi, N. (2012). LPS-Induced Formation of Immunoproteasomes TNF-α and Nitric
468 Oxide Production are Regulated by Altered Composition of Proteasome-Active Sites,
469 *60*, 77–88. https://doi.org/10.1007/s12013-011-9182-8.LPS-Induced

470 Ruan, H., Hacohen, N., Golub, T. R., Parijs, L. Van, & Lodish, H. F. (2002). Tumor Necrosis
471 Factor-α Suppresses Adipocyte-Specific Genes and Activates Expression of
472 Preadipocyte Genes in 3T3-L1 Adipocytes. *Diabetes*, *51*, 1319–1336.

473 Scholz, B., Korn, C., Wojtarowicz, J., Mogler, C., Augustin, I., Boutros, M., … Augustin, H.
474 G. (2016). Endothelial RSPO3 Controls Vascular Stability and Pruning through Non-
475 canonical WNT/Ca2+/NFAT Signaling. *Developmental Cell*, *36*(1), 79–93.
476 https://doi.org/10.1016/j.devcel.2015.12.015

477 Shihabudeen, M. S., Roy, D., James, J., & Thirumurugan, K. (2015). Chenodeoxycholic acid,
478 an endogenous FXR ligand alters adipokines and reverses insulin resistance. *Molecular*
479 *and Cellular Endocrinology*, *414*, 19–28. https://doi.org/10.1016/J.MCE.2015.07.012

480 Shoemaker, L. D., Clark, M. J., Patwardhan, A., Chandratillake, G., Garcia, S., Chen, R., …
481 Steinberg, G. K. (2015). Disease Variant Landscape of a Large Multi-ethnic Population
482 of Moyamoya Patients by Exome Sequencing. *G3 (Bethesda)*, *6*(1), 41–49.
483 https://doi.org/10.1534/g3.115.020321

484 Song, D.-D., Chen, Y., Li, Z.-Y., Guan, Y.-F., Zou, D.-J., & Miao, C.-Y. (2013). Protein
485 tyrosine phosphatase 1B inhibits adipocyte differentiation and mediates TNFα action in
486 obesity. *Biochimica et Biophysica Acta (BBA) - Molecular and Cell Biology of Lipids*,
487 *1831*(8), 1368–1376. https://doi.org/https://doi.org/10.1016/j.bbalip.2013.05.006

488 Song, D. D., Chen, Y., Li, Z. Y., Guan, Y. F., Zou, D. J., & Miao, C. Y. (2013). Protein
489 tyrosine phosphatase 1B inhibits adipocyte differentiation and mediates TNFα action in
490 obesity. *Biochimica et Biophysica Acta - Molecular and Cell Biology of Lipids*, *1831*(8),
491 1368–1376. https://doi.org/10.1016/j.bbalip.2013.05.006

492 Song, G. J., Jung, M., Kim, J., Park, H., Rahman, H., Zhang, S., … Suk, K. (2016). A novel
493 role for protein tyrosine phosphatase 1B as a positive regulator of neuroinflammation.
494 *Journal of Neuroinflammation*, 1–14. https://doi.org/10.1186/s12974-016-0545-3

495 Soromou, L. W., Zhang, Z., Li, R., Chen, N., Guo, W., Huo, M., … Deng, X. (2012).

496 Regulation of Inflammatory Cytokines in Lipopolysaccharide-Stimulated RAW 264.7
497 Murine Macrophage by 7-O-Methyl-naringenin, 3574–3585.
498 https://doi.org/10.3390/molecules17033574

499 Suzuki, J., & Takaku, A. (1969). Cerebrovascular “moyamoya” disease. Disease showing
500 abnormal net-like vessels in base of brain. *Archives of Neurology*, *20*(3), 288–299.
501 https://doi.org/10.1001/archneur.1969.00480090076012

502 Suzuki, S., Mitsuyama, T., Horiba, A., Fukushima, S., Hashimoto, N., & Kawamata, T.
503 (2011). Moyamoya disease complicated by Graves’ disease and type 2 diabetes mellitus:
504 Report of two cases. *Clinical Neurology and Neurosurgery*, *113*(4), 325–329.
505 https://doi.org/10.1016/j.clineuro.2010.11.022

506 Toshihiro Ito, Judith M. Connett, Steven L. Kunkel, and A. M. (2012). Notch system in the
507 linkage of innate and adaptive immunity.

508 Williams, G. (2015). Database of Gene Co-Regulation (dGCR): A Web Tool for Analysing
509 Patterns of Gene Co-regulation across Publicly Available Expression Data. *Journal of*
510 *Genomics*, *3*. https://doi.org/10.7150/jgen.10888

511 Y. H. Lee, S. Nair, E. Rousseau, P. A. Tataranni, C. Bogardus, P. A. Permana, D. B. A. and
512 G. P. P. (2006). Microarray profiling of isolated abdominal subcutaneous adipocytes
513 from obese vs non-obese Pima Indians: increased expression of inflammation-related
514 genes. *Diabetologia*, *48*(9), 1776–1783.

515 Yamauchi, T., Tada, M., Houkin, K., Tanaka, T., Nakamura, Y., Kuroda, S., … Fukui, M.
516 (2000). Linkage of familial moyamoya disease (Spontaneous occlusion of the circle of
517 Willis) to chromosome 17q25. *Stroke*, *31*(4), 930–935.
518 https://doi.org/10.1161/01.STR.31.4.930

519 Zabolotny, J. M., Kim, Y., Welsh, L. A., Kershaw, E. E., Neel, B. G., & Kahn, B. B. (2008).
520 Protein-tyrosine Phosphatase 1B Expression Is Induced by Inflammation in Vivo,
521 *283*(21), 14230–14241. https://doi.org/10.1074/jbc.M800061200

522 Zhou, H., Zhang, X., & Lu, J. (2014). Progress on diabetic cerebrovascular diseases. *Bosnian*
523 *Journal of Basic Medical Sciences*, *14*(4), 185–190.
524 https://doi.org/10.17305/bjbms.2014.4.203

525

Figure Legends

Figure1 Predicted interactome of RNF213. The candidates of the interactome were grouped together in STRING database to visualize their interactions

Figure 2(a) Involvement of predicted interactome in several biological systems. (b) Enrichment process showing the predominance of interactome in immunity and inflammation. (c) Involvement of RNF213 in MHC class I antigen processing. Dynamic areas of RNF213 are encased in pink.

Figure 3 (a) There were four major gene clusters observed to be functioning within the interactome of RNF213. Each color represents a different biological function. **(**b) Treatment of Raw 264.7 cells with LPS induced the expression of TNFα and RNF213 and enhanced expression was noticed after six hours of activation (b) Expression profile of co-regulated members of RNF213 cluster (TRIM21, DTX3L, HERC6) and non-co-regulated member FBXL7 after LPS treatment.

Figure 4 (a)Expression of RNF213 at mRNA level during adipocyte differentiation. RNF213 expressed well during the first 2 days of adipocyte differentiation and on the 8th day. (b) Expression of PTP1Bat mRNA level during adipocyte differentiation. PTP1B expression pattern was similar to that of RNF213.

Figure 5 (a) Effect of pioglitazone on mRNA expression of TNFα and RNF213. LPS stimulated Raw 264.7 cells treated with pioglitazone showed significantly reduced expression of TNFα and slightly reduced expression of RNF213. (b) Expression of RNF213 in 3T3-L1 adipocyte cells treated with pioglitazone. Pioglitazone activates PPARγ which in turn reduced the RNF213 expression.

Figure 6 (a) RNF213 expression in 3T3-L1 adipocytes treated with TNFα. Administration of TNFα (1.5 ng/ml) along with the differentiation media causes a constitutive expression of RNF 213 throughout the adipogenesis process up to 12 days (b) PTP1B expression in 3T3-L1 adipocytes treated with TNFα. Similar to RNF213, the expression of PTP1B was high throughout the adipogenesis process up to 8 days.

Figure 7 Immunoprecipitation was performed with fluorescently labeled antibodies for invitro protein expression analysis a) RNF213 and PTP1B expression in 3T3-L1 adipocyte cells at day 2 of differentiation. **b)** RNF213 and PTP1B expression in TNFα treated adipocytes at day 2 of differentiation. **c)** RNF213 and PTP1B expression in adipocytes at day 5 of differentiation. **d)** RNF213 and PTP1B expression in TNFα treated adipocytes at day 5 of differentiation. The expression of RNF213 and PTP1B was increased by TNFα administration and stayed constitutive during the adipogenesis process. **e)** RNF213 and PTP1B expression in a TNFα and TCS401 co-treated adipocytes at day 5 of differentiation. **f)** RNF213 and PTP1B expression in adipocyte cells at day 2 of differentiation treated with only TCS401.The effect of TNFα on the

constitutive expression of RNF213 was nullified when PTP1B was inactivated. RNF213 was indicated in red colour (Alexa488 tagged antibody), PTP1B was indicated in green colour (Cy3 tagged antibody) and the samples were counterstained with DAPI.

Figure 8 (a) Sodium orthovanadate treatment of adipocytes. Sodium orthovanadate at 35 μM reduced the expression of RNF213 at day 2 of differentiation (b) RNF213 expression in TCS401 treated cells. PTP1B specific inhibitor TCS401 abolished the expression of RNF213 as it inactivated PTP1B at 0.29 μM concentration.

Figure 9(a) Oil Red O staining of adipocytes at day 8 of differentiation. . (**i)** Normal adipogenesis process. (**ii)** TNFα treated cells display less number of lipid droplets indicating reduced adipogenesis. (**iii)** TNFα treated cells with TCS401 co-treatment show enhanced number of lipid droplets suggesting the role of PTP1B on adipogenesis. **b)** Gene expression pattern of PPARγ in adipocytes treated with DIM (differentiation induction media), TNFα, and TCS401. PPARγ expression was gradually increasing and it reached the maximum at day 8 in the cells treated with DIM. PPARγ expression was very low in the cells treated with TNFα. This effect was reversed in cells treated with TCS401.

Figure 10 Oil Red O staining was performed on the 8th day for TCS401 treated differentiated adipocytes. Adipogenesis was increased when PTP1B was inactivated. This was confirmed by the increased levels of PPARγ expression as depicted in Figure 8b

Supplementary data 1. List of interacting molecules to predict a molecular interactome dataset of RNF213

Supplementary data 2.List of forward and reverse primers used in the experiment

Supplementary data 3. Co-regulated members of RNF213 cluster

Supplementary data 4. Curated gene expression data of non-diabetic obese PIMA individuals obtained from Gene Expression Omnibus

Figure 1

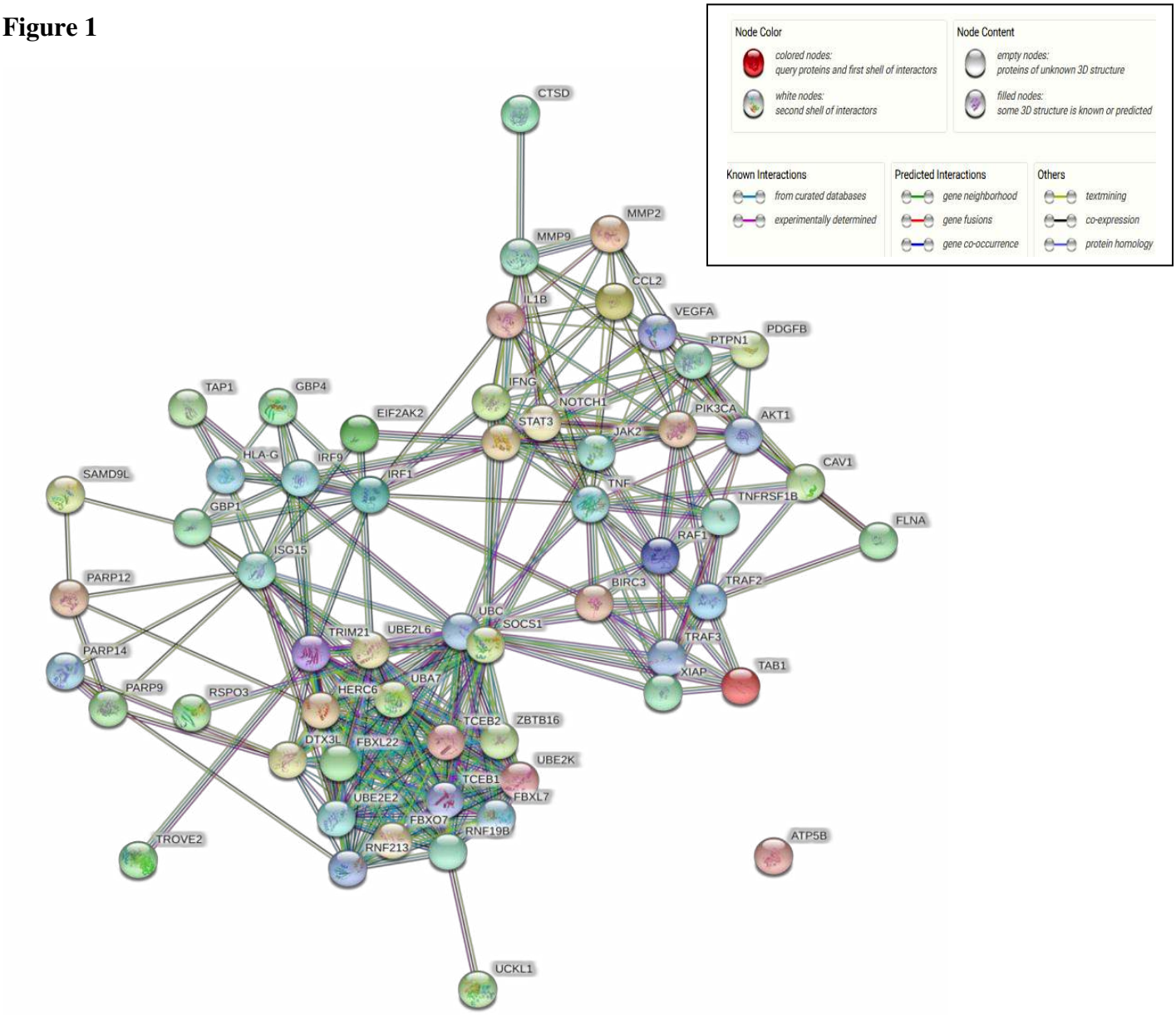
Node Color
colored nodes:
query proteins and first shell of interactors
white nodes:
second shell of interactors
Node Content
empty nodes:
proteins of unknown 3D structure
filled nodes:
some 3D structure is known or predicted
Known Interactions
from curated databases
experimentally determined
Predicted Interactions
gene neighborhood
gene fusions
gene co-occurrence
Others
textmining
co-expression
protein homology
CTSD
MMP2
MMP9
CCL2
IL1B
VEGFA
PDGFB
PTPN1
TAP1
GBP4
IFNG
NOTCH1
EIF2AK2
STAT3
PIK3CA
AKT1
JAK2
HLA-G
IRF9
IRF1
CAV1
SAMD9L
TNF
TNFRSF1B
GBP1
FLNA
RAF1
ISG15
PARP12
BIRC3
TRAF2
UBC
SOCS1
TRIM21
UBE2L6
TRAF3
PARP14
TAB1
XIAP
UBA7
PARP9
RSPO3
HERC6
TCEB2
ZBTB16
DTX3L
FBXL22
UBE2K
TCEB1
UBE2E2
FBXL7
FBXO7
RNF19B
TROVE2
RNF213
ATP5B
UCKL1

Figure 2

(a)

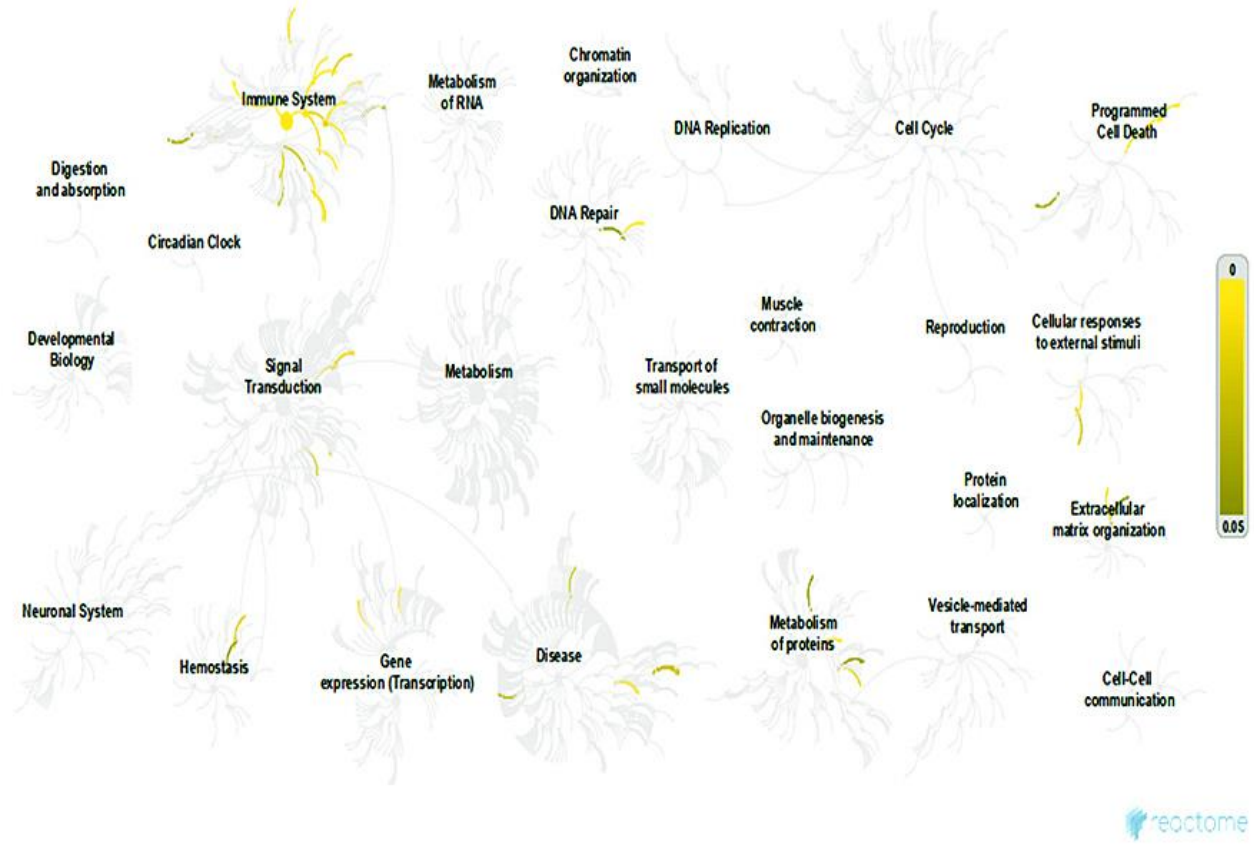
Immune System
Metabolism of RNA
Chromatin organization
DNA Replication
Cell Cycle
Programmed Cell Death
Digestion and absorption
DNA Repair
Circadian Clock
Muscle contraction
Reproduction
Cellular responses to external stimuli
Developmental Biology
Signal Transduction
Metabolism
Transport of small molecules
Organelle biogenesis and maintenance
Protein localization
Extracellular matrix organization
Neuronal System
Hemostasis
Gene expression (Transcription)
Disease
Metabolism of proteins
Vesicle-mediated transport
Cell-Cell communication
0
0.05
reactome

(b)

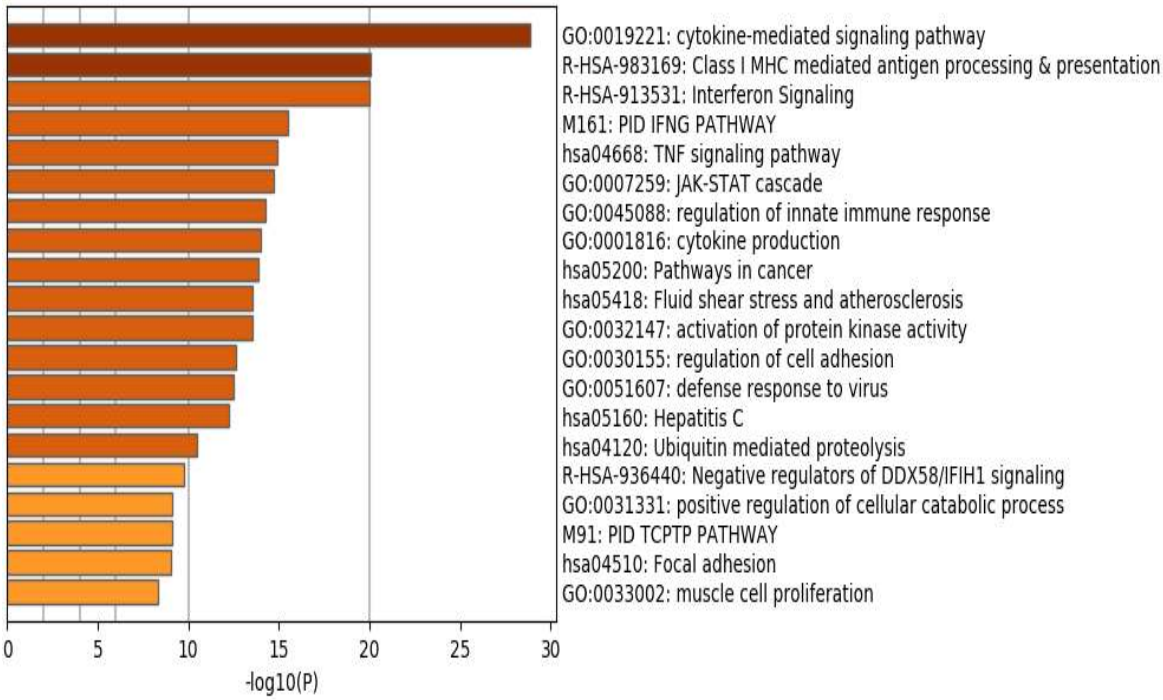
GO:0019221: cytokine-mediated signaling pathway
R-HSA-983169: Class I MHC mediated antigen processing & presentation
R-HSA-913531: Interferon Signaling
M161: PID IFNG PATHWAY
hsa04668: TNF signaling pathway
GO:0007259: JAK-STAT cascade
GO:0045088: regulation of innate immune response
GO:0001816: cytokine production
hsa05200: Pathways in cancer
hsa05418: Fluid shear stress and atherosclerosis
GO:0032147: activation of protein kinase activity
GO:0030155: regulation of cell adhesion
GO:0051607: defense response to virus
hsa05160: Hepatitis C
hsa04120: Ubiquitin mediated proteolysis
R-HSA-936440: Negative regulators of DDX58/IFIH1 signaling
GO:0031331: positive regulation of cellular catabolic process
M91: PID TCPTP PATHWAY
hsa04510: Focal adhesion
GO:0033002: muscle cell proliferation
0
5
10
15
20
25
30
-log10(P)

(c)

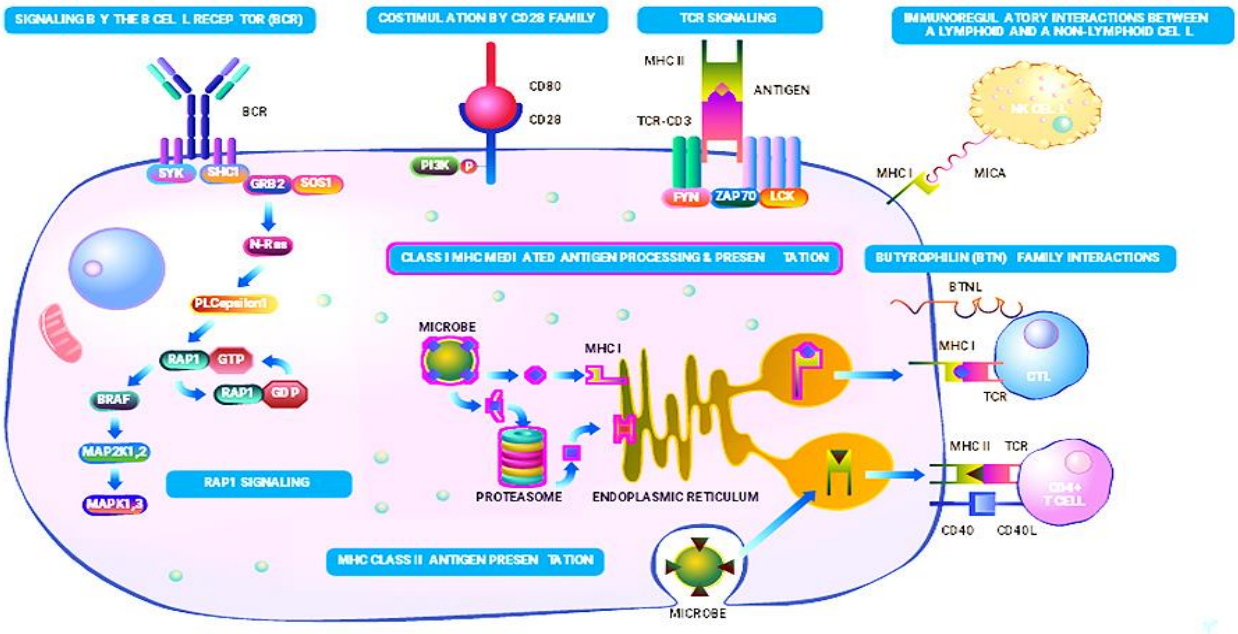
SIGNALING BY THE B CELL RECEPTOR (BCR)
COSTIMULATION BY CD28 FAMILY
TCR SIGNALING
IMMUNOREGULATORY INTERACTIONS BETWEEN A LYMPHOID AND A NON-LYMPHOID CELL
BCR
SYK
SHC1
GRB2
SOS1
N-Ras
PLCepsilon1
RAP1
GTP
RAP1
GDP
BRAF
MAP2K1,2
MAPK1,3
RAP1 SIGNALING
CD80
CD28
PI3K
P
MHC II
ANTIGEN
TCR-CD3
FYN
ZAP70
LCK
MHC I
MICA
CLASS I MHC MEDIATED ANTIGEN PROCESSING & PRESENTATION
MICROBE
MHC I
PROTEASOME
ENDOPLASMIC RETICULUM
MHC CLASS II ANTIGEN PRESENTATION
MICROBE
BUTYROPHILIN (BTN) FAMILY INTERACTIONS
BTNL
MHC I
TCR
CTL
MHC II
TCR
CD4+ T CELL
CD40
CD40L

Figure 3

(a)

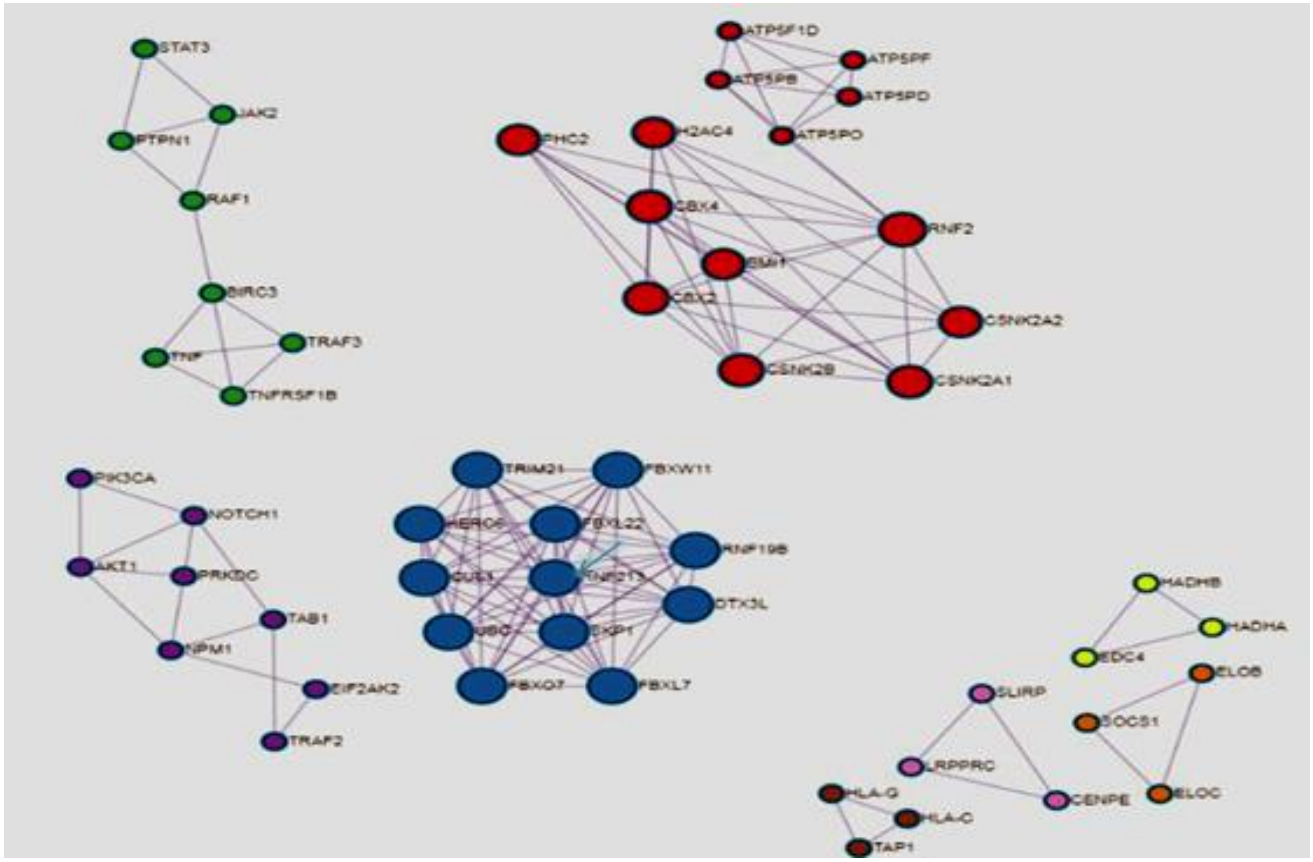
STAT3
JAK2
PTPN1
TRAF1
BIRC3
TRAF3
TNF
TNFRSF1B
ATP5F1D
ATP5PF
ATP5PB
ATP5PD
ATP5PO
PHC2
H2AC4
CBX4
RNF2
BMI1
CBX2
CSNK2A2
CSNK2B
CSNK2A1
PIK3CA
NOTCH1
AKT1
PRKDC
TAB1
NPM1
EIF2AK2
TRAF2
TRIM21
FBXW11
HERC5
FBXL22
RNF19B
GUK1
RNF213
OTX3L
UBC
EXOSC1
FBXO7
FBXL7
HADHB
HADHA
EDC4
ELOB
SLIRP
SOCS1
LRPPRC
ELOC
HLA-G
CENPE
HLA-C
TAP1

(b)

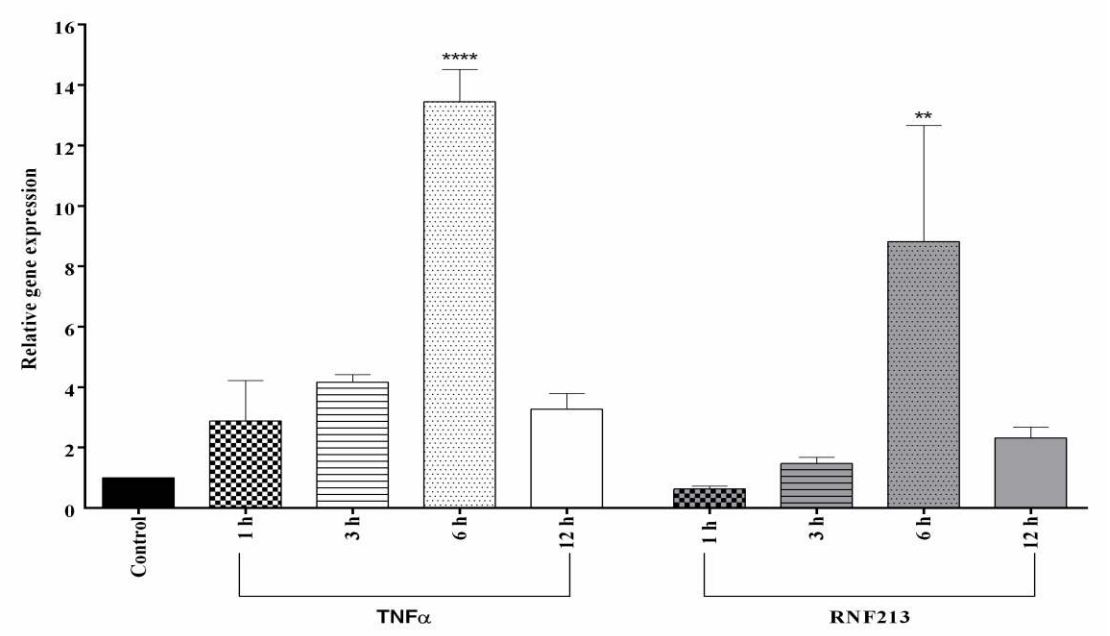
Relative gene expression
16
14
12
10
8
6
4
2
0
****
**
Control
1 h
3 h
6 h
12 h
1 h
3 h
6 h
12 h
TNFα
RNF213

(c)

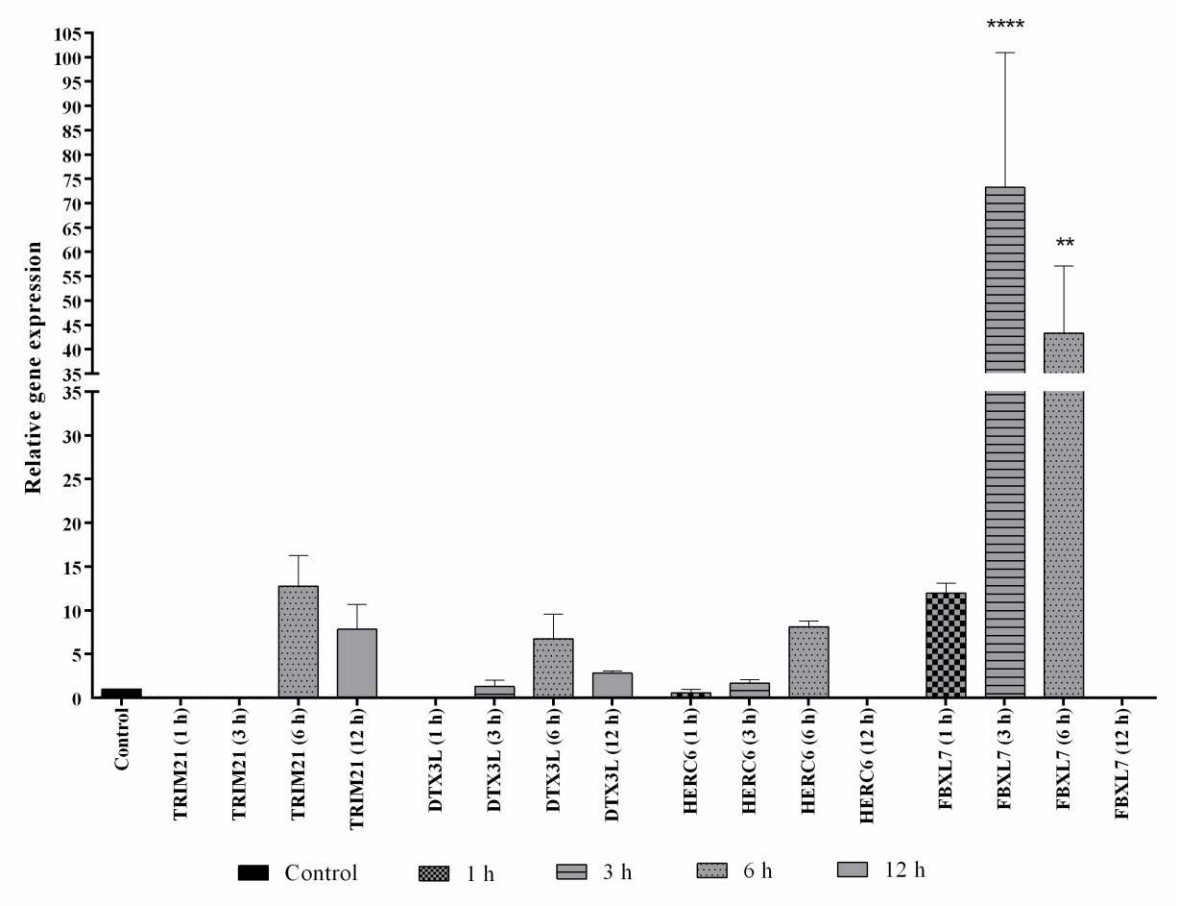
Relative gene expression
105
100
95
90
85
80
75
70
65
60
55
50
45
40
35
30
25
20
15
10
5
0
****
**
Control
TRIM21 (1 h)
TRIM21 (3 h)
TRIM21 (6 h)
TRIM21 (12 h)
DTX3L (1 h)
DTX3L (3 h)
DTX3L (6 h)
DTX3L (12 h)
HERC6 (1 h)
HERC6 (3 h)
HERC6 (6 h)
HERC6 (12 h)
FBXL7 (1 h)
FBXL7 (3 h)
FBXL7 (6 h)
FBXL7 (12 h)
Control
1 h
3 h
6 h
12 h

Figure 4

(a)

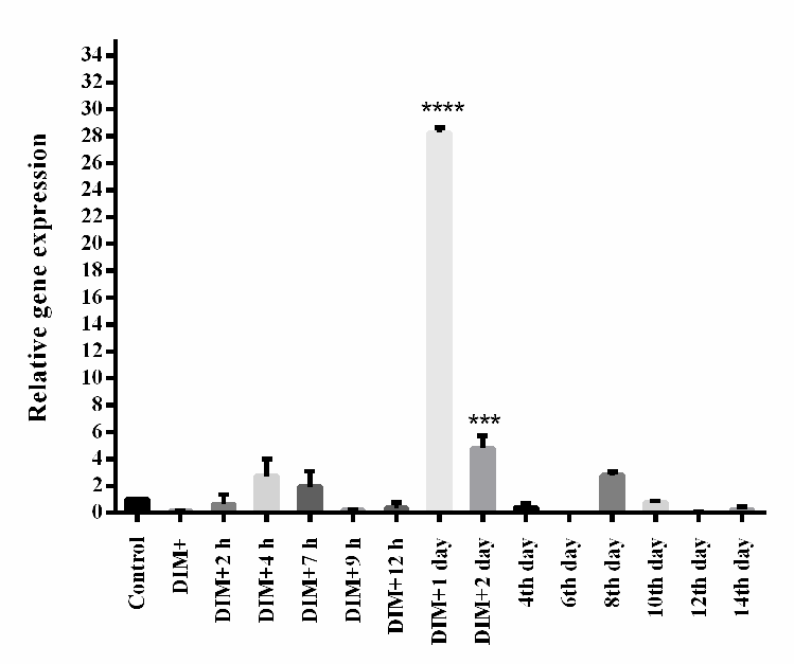
Relative gene expression
****
***
Control
DIM+
DIM+2 h
DIM+4 h
DIM+7 h
DIM+9 h
DIM+12 h
DIM+1 day
DIM+2 day
4th day
6th day
8th day
10th day
12th day
14th day

(b)

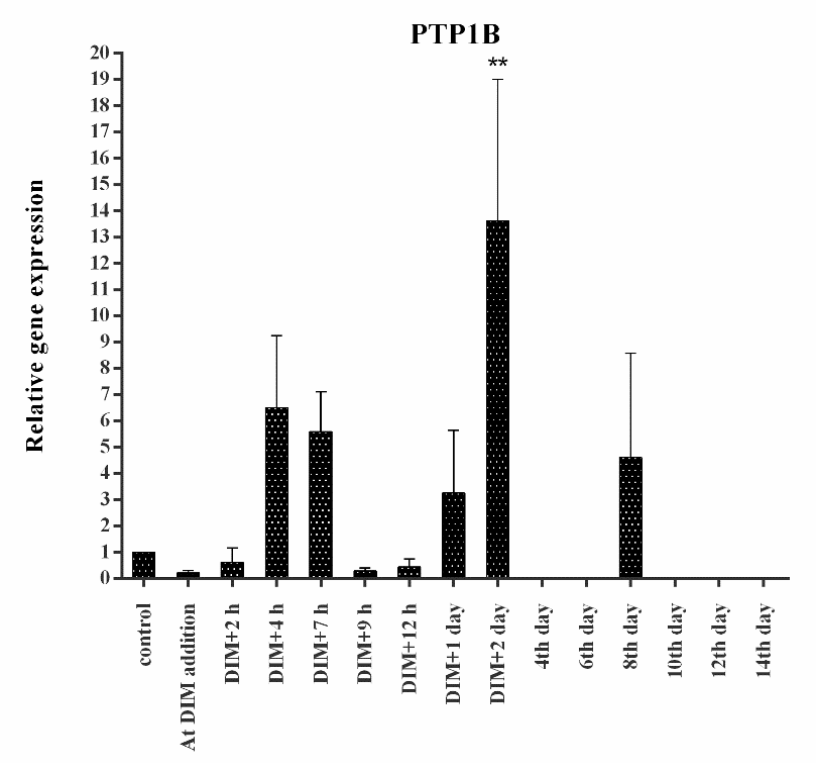
PTP1B
Relative gene expression
**
control
At DIM addition
DIM+2 h
DIM+4 h
DIM+7 h
DIM+9 h
DIM+12 h
DIM+1 day
DIM+2 day
4th day
6th day
8th day
10th day
12th day
14th day

Figure 5

(a)

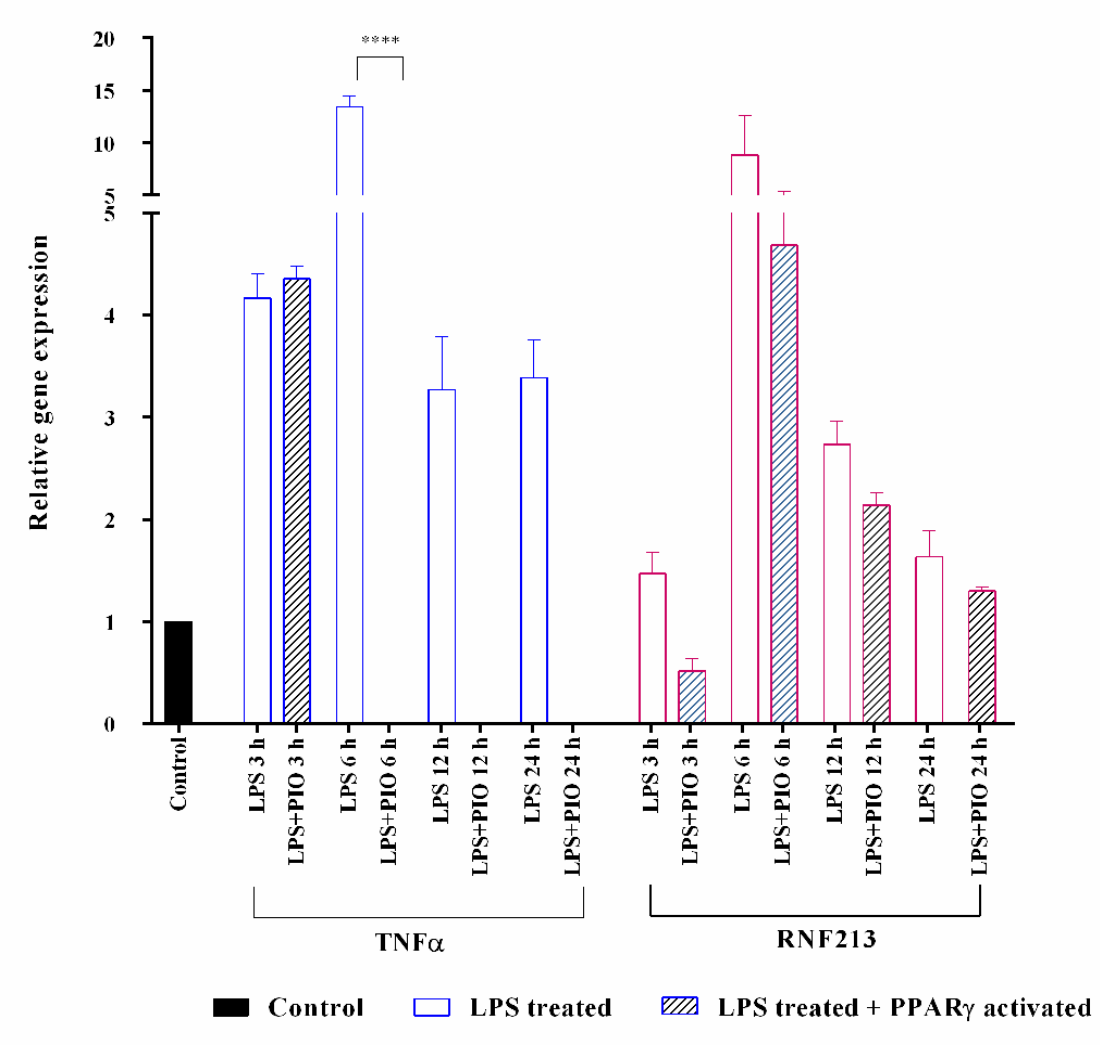
Relative gene expression
20
15
10
5
4
3
2
1
0
****
Control
LPS 3 h
LPS+PIO 3 h
LPS 6 h
LPS+PIO 6 h
LPS 12 h
LPS+PIO 12 h
LPS 24 h
LPS+PIO 24 h
LPS 3 h
LPS+PIO 3 h
LPS 6 h
LPS+PIO 6 h
LPS 12 h
LPS+PIO 12 h
LPS 24 h
LPS+PIO 24 h
TNFα
RNF213
Control
LPS treated
LPS treated + PPARγ activated

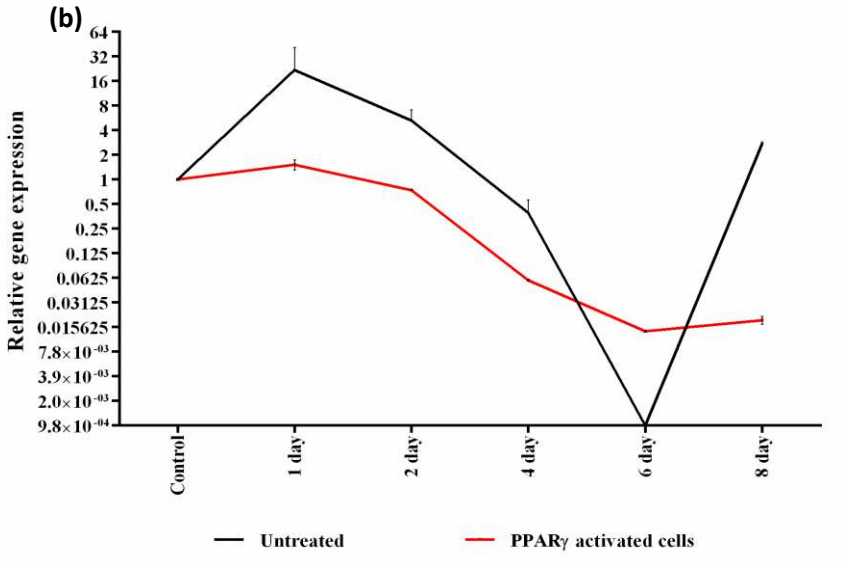
(b)
Relative gene expression
64
32
16
8
4
2
1
0.5
0.25
0.125
0.0625
0.03125
0.015625
7.8×10-03
3.9×10-03
2.0×10-03
9.8×10-04
Control
1 day
2 day
4 day
6 day
8 day
Untreated
PPARγ activated cells

Figure 6

(a)

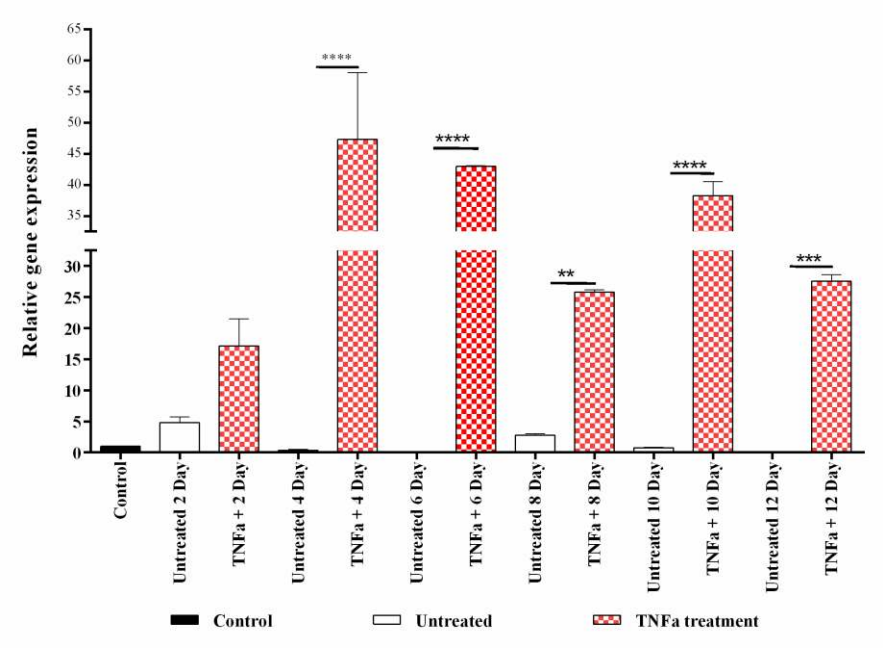
Relative gene expression
65
60
55
50
45
40
35
30
25
20
15
10
5
0
****
****
****
**
***
Control
Untreated 2 Day
TNFa + 2 Day
Untreated 4 Day
TNFa + 4 Day
Untreated 6 Day
TNFa + 6 Day
Untreated 8 Day
TNFa + 8 Day
Untreated 10 Day
TNFa + 10 Day
Untreated 12 Day
TNFa + 12 Day
Control
Untreated
TNFa treatment

(b)

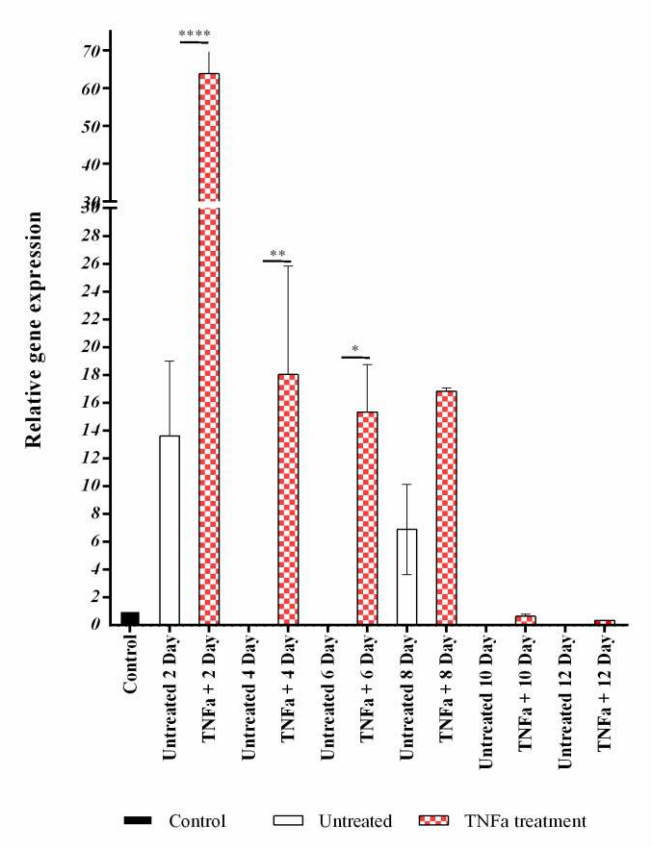
Relative gene expression
70
60
50
40
30
28
26
24
22
20
18
16
14
12
10
8
6
4
2
0
****
**
*
Control
Untreated 2 Day
TNFa + 2 Day
Untreated 4 Day
TNFa + 4 Day
Untreated 6 Day
TNFa + 6 Day
Untreated 8 Day
TNFa + 8 Day
Untreated 10 Day
TNFa + 10 Day
Untreated 12 Day
TNFa + 12 Day
Control
Untreated
TNFa treatment

Figure 7

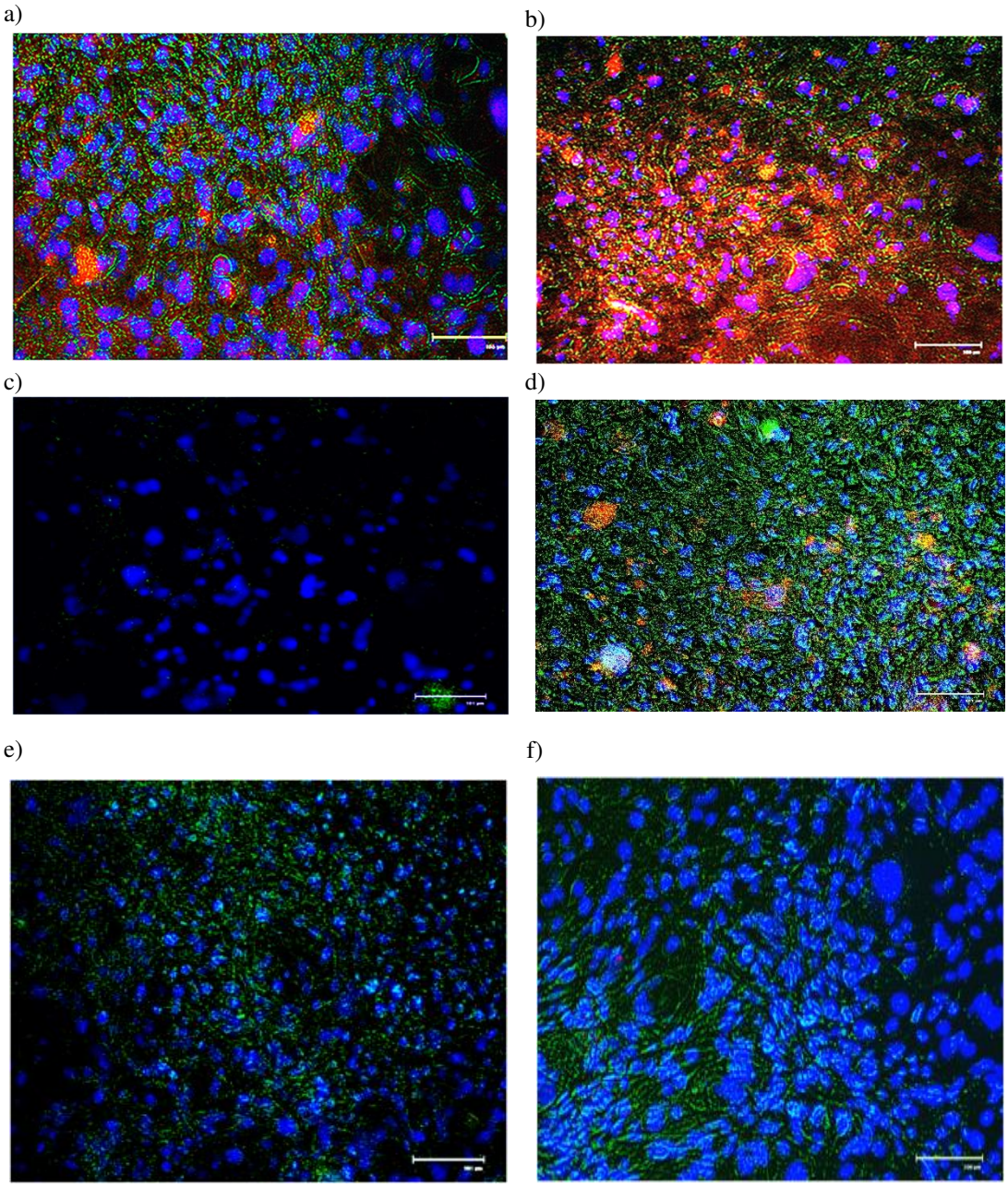

Figure 8

(a)

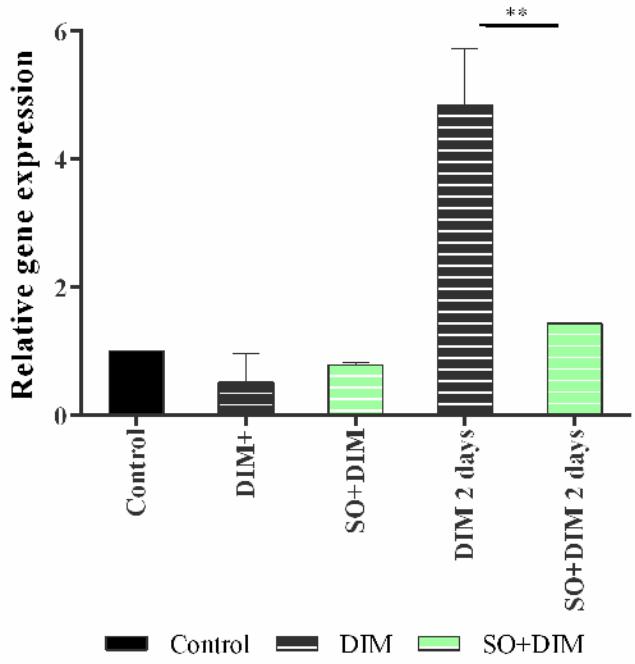
Relative gene expression
6
4
2
0
**
Control
DIM+
SO+DIM
DIM 2 days
SO+DIM 2 days
Control
DIM
SO+DIM

(b)

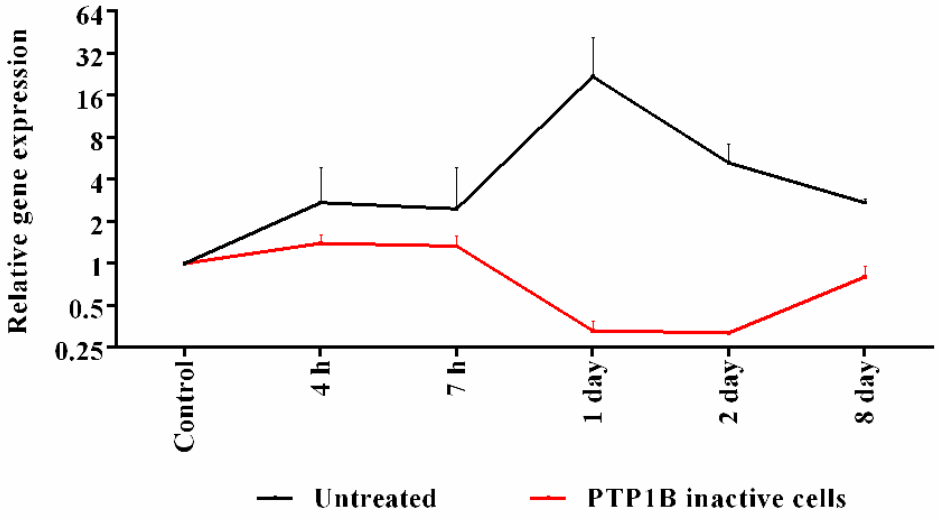
Relative gene expression
64
32
16
8
4
2
1
0.5
0.25
Control
4 h
7 h
1 day
2 day
8 day
Untreated
PTP1B inactive cells

Figure 9

(a)

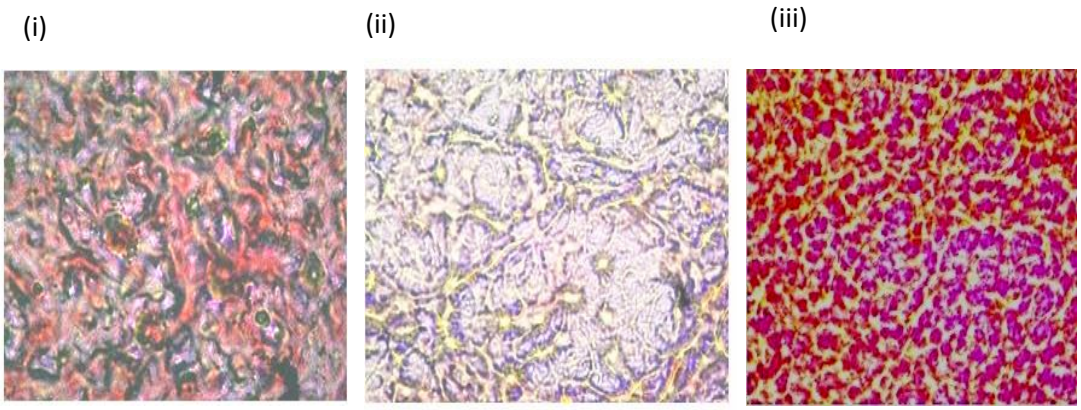
(i)
(ii)
(iii)

(b)

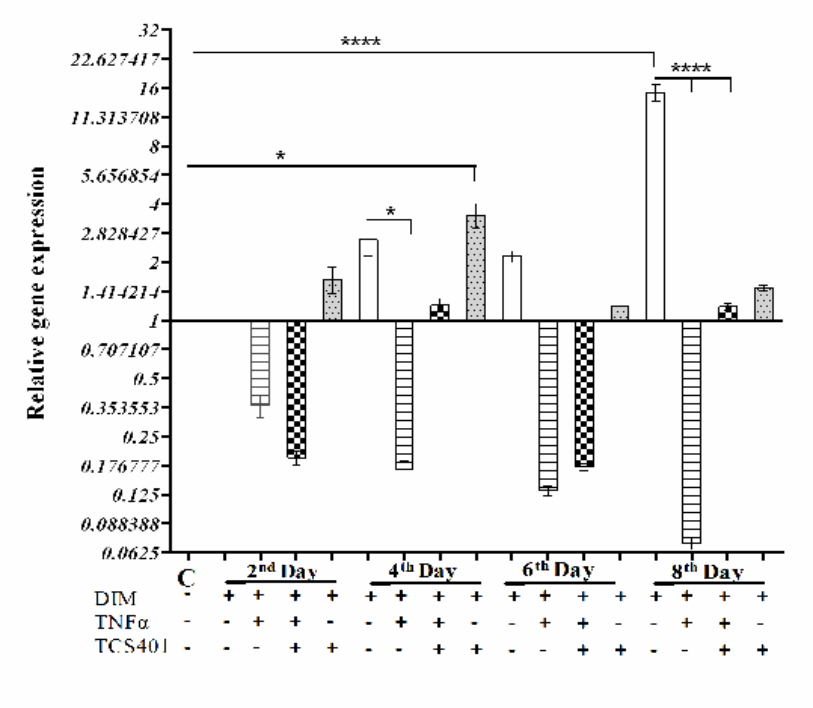
Relative gene expression
32
22.627417
16
11.313708
8
5.656854
4
2.828427
2
1.414214
1
0.707107
0.5
0.353553
0.25
0.176777
0.125
0.088388
0.0625
****
****
*
*
C
2nd Day
4th Day
6th Day
8th Day
DIM
TNFα
TCS401

Figure10

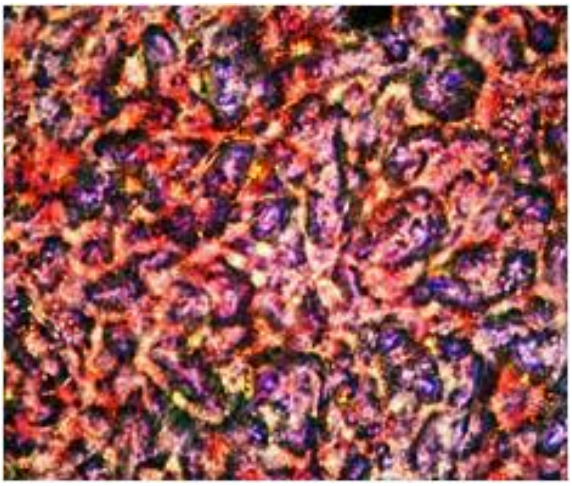

Normal 8th day

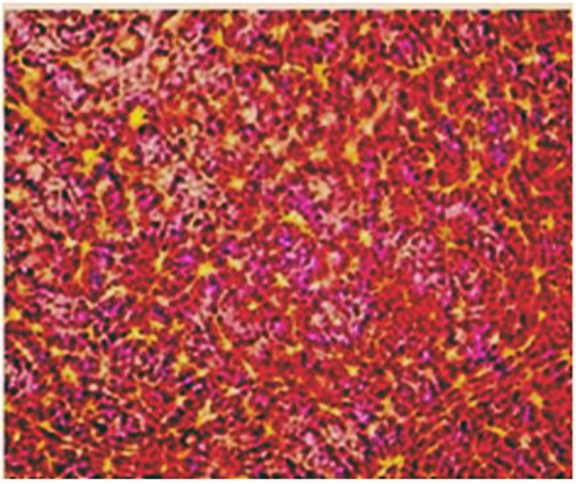

TCS401 treated 8th day

Strategy for interactome prediction